Astronomical and Astrophysical Transactions (*AApTr*), 2025, Vol. 35, Issue 1, pp. 1–16,
ISSN 1055-6796, Photocopying permitted by license only, ©Cambridge Scientific Publishers

Ultra-cool brown dwarfs with and without circum-substellar plasma disks: possible consequences

E.S. Belenkaya[1,*], I.I. Alexeev[1], G.P. Malygin[1,2]

[1]*FSBEIHE M.V. Lomonosov Moscow State University, Skobeltsyn Institute of Nuclear Physics, 1(2) Leninskie Gory, GSP-1, Moscow 119991, Russian Federation*
[2]*FSBEIHE M.V. Lomonosov Moscow State University, Faculty of Physics, Leninskie Gory, Moscow 119991, Russian Federation*

Received 12 March, 2025; accepted 24 April, 2025

We analyze the literature data for two isolated Y-type brown dwarfs: CWISEP J1935 18.59-154620.3 (W1935 for short) and WISE J222055.31-362817.4 (W2220 for short) with close masses, similar radii, temperatures, solar luminosity ratios, and chemical compositions, however, the CH_4 infrared emission was detected only from one of them (W1935), but not from the other (W2220). It was also found that W2220 does not have a temperature inversion with atmospheric altitude, while W1935 does. We suggest that the possible reason for this is that the brown dwarf W1935 has its own magnetic field and a surrounding plasma current disk (or magnetodisk), while W2220 does not.

Keywords: Brown dwarfs, infrared emission, magnetodisk, aurora

1 Introduction

Brown dwarfs, which are celestial bodies intermediate between stars and planets, are generally considered to have masses ranging from ∼13 to ∼80 M_J, where $M_J = 1.9 \times 10^{27}$ kg is the mass of Jupiter. The upper limit (80 M_J) is the mass at which thermonuclear reactions with hydrogen combustion occur in the cores of the celestial bodies, while the lower one (13 M_J) is the deuterium-burning limit.

Faherty et al. (2024) described two isolated ultra-cool Y-class brown dwarfs, CWISEP J193518.59-154620.3 (W1935 for short) and WISE J222055.31-362817.4 (W2220 for short), with masses ranging from 6 to 35 M_J. Objects with masses less than 13 M_J are called sub-brown dwarfs or planetary-mass brown dwarfs. They form in the same way as stars and brown dwarfs: by the collapse of a gas cloud, but their mass is below the limiting mass for deuterium fusion ($<13M_J$). Brown dwarfs W1935 and W2220 are near clones, as they have similar parameters.

*Email: elena.belenkaya.msu@gmail.com

Sub-brown dwarf W1935. The distance from the Sun is 14.4 pc (47.06 light years); mass, about 1.5% of the solar mass or 10.5 M_J; the radius is about the radius of Jupiter; temperature, ∼482 K; age, ∼4.5 billion years (https://www.stellarcatalog.com/stars/cwisep-j1935–1546). NASA's James Webb Space Telescope found infrared emission from methane at this object. According to Faherty et al. (2024) its temperature is ∼300 K, which we will take into account here.

Sub-brown dwarf W2220. The distance from the Sun is 11.5 pc (37.4 light years); mass, about 2% of the solar mass or 21 M_J; radius, about the radius of Jupiter; temperature, ∼480K; age, ∼4.5 billion years (https://www.stellarcatalog.com/stars/cwisep-j1935–1546).

Faherty et al. (2024) drew attention to the fact that, despite similar sizes, close masses, chemical compositions, and luminosities, there is a difference in the spectral characteristics of these brown dwarfs. While W2220 exhibits CH_4 q-branch absorption centered at 3.326 μm, W1935 emits in the same wavelength range (3.25–3.45 μm). Both dwarfs are isolated; no stars, planets, or satellites have been detected near them.

Faherty et al. (2024) concluded that the atmospheric temperature for W2220 decreases with altitude, as is typical of isolated brown dwarfs, but for W1935 the atmospheric temperature increases with altitude and reaches approximately 300 K at a pressure of 1–10 mbar. The temperature inversion in the atmosphere of W1935 is accompanied by CH_4 emission. When analyzing the data, Faherty et al. (2024) assumed the absence of clouds in the atmosphere. They wondered how a temperature inversion in the stratosphere of an isolated dwarf is possible in the absence of an irradiating star. We will try to answer the questions about the different behavior of these twin brown dwarfs.

Why one of two isolated sub-brown dwarfs with similar characteristics exhibits strong methane emission and atmospheric temperature inversion with altitude, while the other does not, is an actual question important for understanding the processes occurring in these objects and their surroundings.

In Section 2 we consider the evolution of brown dwarfs during their lifetime on the density-temperature diagram for M stars, giant planets and brown dwarfs. Section 3 describes our assumption of the existence of a current disk around the brown dwarf W1935 and its absence in the environment of W2220 as a possible explanation for these observations. In Section 4 we offer a description of a possible mechanism for generating polar emissions at W1935. Section 5 presents the suggested current system and corresponding formulas. Section 6 proposes a possible cause for the temperature inversion, and Section 7 presents conclusions.

2 Temperature–density relationship for brown dwarfs, M-dwarfs and giant planets

Here we briefly consider how brown dwarfs evolve during their life and compare their characteristics with similar properties of red dwarfs (stars) and gas giants. The main parameters for comparing celestial bodies are mass, radius, density and effective temperature (i.e. calculated theoretically using the black body approximation). For exoplanets, the effective temperature is achieved mainly by heating from their host stars.

In this work we examine the relationship between temperature and density for these three types of celestial bodies. For example, the relationships between density and mass of low-mass planets, brown dwarfs, gas giants and stars were investigated by Persson et al. (2019) while studying the brown dwarf desert.

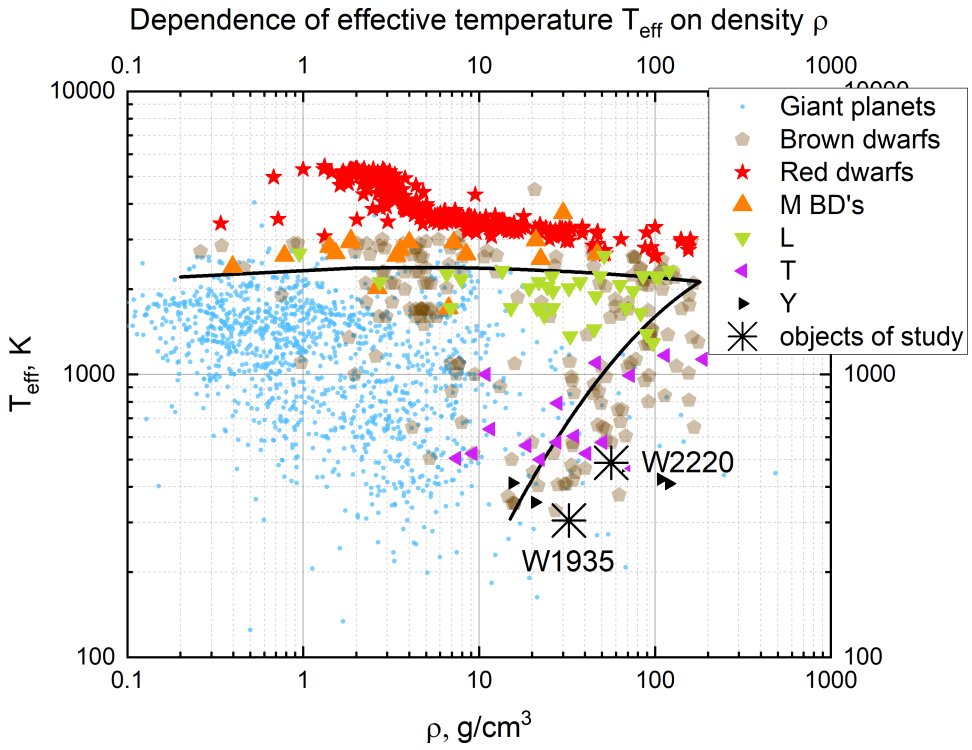


Figure 1 The graph highlights brown dwarfs for which the spectral class is known. In the background there are all brown dwarfs (in brown), for which two characteristics are known: temperature and density. The black curves are polynomial approximations of the most common brown dwarfs with these parameters on a logarithmic scale. Two ultra-cool brown dwarfs W1935 and W2220 discussed in this paper are shown by asterisks. Parameters of brown dwarfs were taken from https://johnstonsarchive.net/astro/browndwarflist.html; and parameters of gas giant planets and red dwarfs were taken from https://exoplanetarchive.ipac.caltech.edu/.

In Fig. 1 two regions can be visually distinguished where many brown dwarfs are concentrated: a horizontal region with temperatures from 2000 K to 3000 K and densities from 0.1 g/cm^3 to 200 g/cm^3, and a sloping region on the right with temperatures from 300 K to 3000 K and densities from 10 g/cm^3 to 200 g/cm^3. These regions were roughly approximated by second-order polynomials in logarithmic scale (Fig. 1, black curves).

Figure 1 shows how brown dwarfs are divided into two main groups. The first, located horizontally, lies between planets and stars. This group corresponds to the definition of a brown dwarf, which states that it is a substellar object, often called

a "failed" star. The spectral classes of brown dwarfs allow us to analyze an indirect estimate of their age. Old brown dwarfs are located mainly at the second black curve.

According to the theory of evolution, brown dwarfs burn their fuel relatively quickly and cool down over time (Cushing et al., 2011). As they cool, they change their spectral class, starting with M-class early in their lives, corresponding to the hottest brown dwarfs, and ending with Y-class, corresponding to the oldest and coolest dwarfs. This means that knowing the spectral class of a brown dwarf, we can infer its age. Figure 1 shows how brown dwarfs "move" as time progresses from the upper left corner to the upper right with almost constant temperature and increasing density and after that to the lower right corner in the direction of sharp decreasing of temperature and density along black arc.

Formation of M-class brown dwarfs. At the beginning of their lives, high-temperature brown dwarfs are most similar in their properties to stellar red dwarfs. Brown dwarfs form in a similar way to stars, from a cloud of gas and dust, but in the case of brown dwarfs they are not massive enough to form stars that sustain hydrogen burning in their cores. However, it is also possible that during the formation of a brown dwarf, the temperature rises so high for some time that it exceeds the temperature of main sequence stars. In this case, the brown dwarf may be mistakenly identified as a star. At this stage of its life, a brown dwarf may behave like a very faint red dwarf (Gerasimov et al., 2024).

Deuterium burning (L-class brown dwarfs). Upon transitioning to the L-class, brown dwarfs begin to gradually cool down and reach their maximum density. After the initial stage of brown dwarf formation, deuterium burning persists. Deuterium is less abundant in the universe than hydrogen; moreover, it burns relatively quickly within a brown dwarf. If the brown dwarf was initially low mass, the deuterium may not burn at all, remaining largely untouched (Luhman, 2014).

Methane formation (T-class brown dwarfs). As time progresses, brown dwarfs move along the inclined right-hand arc (Fig. 1). The movement is accompanied by a further accelerated decrease in temperature and density. This arc corresponds to the cessation of deuterium burning reactions within the brown dwarf. After all thermonuclear reactions have ceased, the brown dwarf's temperature begins to drop even faster. When it reaches 1000 K, methane begins to form in the upper layers of the atmosphere, which is reflected in the spectrum of the brown dwarf. The brown dwarf still emits a faint red light in the visible diapason (Faherty et al., 2024).

Last stage of evolution (Y-class brown dwarfs). When a brown dwarf has cooled enough that it no longer emits visible light, it reaches equilibrium. In this state, a brown dwarf resembles a gas giant more than a star. The difference is that while their radii are almost the same or sometimes smaller than those of a gas giant, the dwarf's mass on average exceeds the mass of the planets. Gas giants and brown dwarfs also have different chemical compositions. At this stage of life, ammonia appears in the brown dwarf's atmosphere (Robbins et al., 2023). We see from Fig. 2 that two sub-brown dwarfs considered in this paper are very old, cool and have a relatively large density.

3 The assumption of the existence of a current disk around the brown dwarf W1935

To explain the difference in characteristics of these twin brown dwarfs, we can assume that there is interstellar plasma around W1935, which formed a circum-substellar plasma disk. If this sub-brown dwarf has a magnetic field and rotates rapidly, then when the magnetic field lines move through a conducting plasma, a unipolar induced EMF can arise in the presence of differential rotation caused by radial outflow in the disk.

Kobyakov (2023) studied the plasma environment of brown dwarfs and the interchange instability acting in it in the case of rapid rotation. He noted that typical values of the dipole magnetic field on the surface of brown dwarfs are of the order of 10^3–10^4 G. He also emphasized the significant role of the Alfvén radius in the process of formation of a plasma disk around a brown dwarf with a sufficient amount of magnetospheric plasma and the presence of a conducting surface on the celestial body. Nakajima (1985) considered the possibility of disk formation around the magnetic rotating star Sigma Orionis E. Climent et al. (2023) noted that many ultra-cool brown dwarfs have radiation belts in their plasma environment and aurora as at Jupiter.

In the Solar System, the most typical representative of a planet with a magnetodisk is Jupiter, with which brown dwarfs are often compared. Jupiter's magnetodisk is associated with the braking of the rigid corotation of the magnetospheric plasma due to the radial outflow in the equatorial plane under the action of centrifugal force (see, for example, Hill, 1980; Cowley et al., 2003).

Scholz et al. (2018) observed, on average, a linear increase in the characteristic rotation period of young brown dwarfs with increasing mass. Old brown dwarfs (3–10 million years) rotated faster, possibly due to contraction and conservation of angular momentum. As the brown dwarfs considered here are rather old (∼4.5 billion years), we can suppose their fast rotation.

Bespalov and Savina (2018) noted that ultra-cool brown dwarfs can generate coherent radio emission if they have a large-scale constant magnetic field of the order of kG. The generation mechanism of radio emission is kinetic cyclotron instability. Reiners and Christensen (2010) estimated the magnetic field of the brown dwarfs assuming their fast rotation. They obtained values from several kG to ∼100 G with increasing age for massive brown dwarfs.

Nichols et al. (2012) drew an analogy between ultra-cool, rapidly rotating brown dwarfs and Jupiter. If the dwarf's magnetic field is rather strong and there is enough plasma in the disk around it, powerful field-aligned currents will flow from the ionosphere into the equatorial plane of the magnetosphere, where the rigid corotation of the magnetospheric plasma is disrupted by radial outflow. This will result in radio emission from brown dwarf like in the case of Jupiter, which implies as the underlying mechanism the electron cyclotron maser instability (CMI). Hallinan et al. (2008) showed that CMI is the dominant mechanism generating radio emission in the magnetospheres of ultra-cool dwarfs. This radio emission is circularly polarized.

We also consider the hypothesis of the existence of a circum-substellar plasma disk around the ultra-cool, rapidly rotating magnetic Y-class brown dwarf W1935 and assume its absence, or/and the absence of an intrinsic magnetic field for W2220. Based on this assumption, we show that polar auroras and temperature inversion with

altitude in the atmosphere will occur for W1935, while these phenomena should not be observed for W2220. For rough estimates, we assume that the magnetic field of the brown dwarf W1935 is perpendicular to its rotational equator (see also the same assumption in Hill, 2001 and Nichols et al., 2012).

4 Possible cause of auroras on W1935

The study of celestial bodies in the Solar System has shown that powerful discrete auroras in ovals arise for two reasons: 1) during the interaction with the plasma flow passing by (stellar/solar wind or magnetospheric plasma); 2) as a result of the action of unipolar induction. The first mechanism is responsible for auroras in ovals on Earth and Saturn, as well as in the roots of field lines passing through the Galilean satellites of Jupiter (Neubauer, 1980; Wright and Southwood, 1987; Alexeev and Belenkaya, 1991; Kivelson et al., 1996). The second mechanism explains the generation of the main ovals on Jupiter (Hill, 2001; Cowley et al., 2003; Alexeev, Belenkaya, 2005; Belenkaya, 2004). How the first mechanism acts at exoplanets causing auroral radio emission is described, for example, in the work of Nichols and Milan (2016). For the second mechanism to work, the presence of a plasma current disk, surrounding a rapidly rotating magnetic celestial body, is necessary.

Considering an analogy between Jupiter and brown dwarfs, Kobyakov (2023) drew attention to the discrepancy between the observed rate of the radial outflow in the plasma disk around Jupiter and the velocity predicted by the interchange instability, which is often used to describe plasma dynamics in the magnetospheres of giant planets in the Solar System.

The question of the possible generation of aurora emission by an isolated brown dwarf is considered in detail in the work of Nichols et al. (2012). It is noted there that circularly polarized radio emissions have been recorded from ultra-cool brown dwarfs, caused by electron cyclotron maser instability. An analogy is drawn with Jupiter, for which such radio emission is associated with strong field-aligned currents in the regions of the main polar ovals.

Saur et al. (2021) considered the cause of auroras on the brown dwarf 2MASS J1237+6526. The authors showed that rapidly rotating magnetic brown dwarfs can generate UV auroras with a power of 10^{19} W or more. As noted by Saur et al. (2021), very little is known about the properties of the plasma environment of brown dwarfs. Based on observations, several brown dwarfs were estimated to have a magnetic field of about 10^3–10^4 G and an angular rotation velocity of $\sim 10^{-3}$ radians per second (Saur et al., 2021, Figure 1). Kao et al. (2018) recorded circularly polarized radio emission from the polar regions of brown dwarfs, from which they determined their minimum average surface magnetic field of ∼2.3–4.4 kG. They found that the age dependence of the brown dwarf's dynamo mechanism is weak. Saur et al. (2021), assuming that the properties of the interstellar medium around brown dwarfs are approximately the same as near the heliopause, showed that their magnetosphere has very large dimensions $> 740\ R_{bd}$ (R_{bd} is the radius of the brown dwarf).

Radio emissions from magnetic fast-rotating isolated brown dwarfs (Nichols et al., 2012), as well as from exoplanets (Nichols and Milan, 2016), can be expected to be

measured if they are excited by CMI, generating coherent, powerful auroral radio emissions. This has been observed from brown dwarfs, but not from exoplanets yet.

Here we consider the conditions under which auroras on an isolated ultra-cool, rapidly rotating magnetic brown dwarf could be caused by its interaction with the surrounding plasma environment. To explain the observed auroras, we assume that W1935 has a strong magnetic field, rapid rotation, and a circum-substellar current disk with enough plasma.

5 Results

Polar auroras on a magnetic rotating isolated brown dwarf can be excited by magneto-spheric-ionospheric interaction with the plasma disk. If there is enough plasma in it, starting from a certain distance the dipole field lines cannot hold it longer, and under the action of the centrifugal force the radial outflow begins. We consider that this distance is of the order of the Alfvén radius, R_A, at which the kinetic and magnetic energy densities are equal (Khodachenko et al. (2012); Belenkaya and Khodachenko, 2012). At this distance the Alfvén Mach number M_A is equal to 1: $M_A = V_{pl}/V_A = 1$, where V_{pl} is the plasma flow velocity, and V_A is the Alfvén velocity in the disk.

At distance $r < R_A$ the magnetic energy density is higher than the kinetic energy density and the magnetic field determines the plasma motion along the magnetic field lines; at $r > R_A$, on the contrary, the kinetic energy density dominates, and the plasma radial outflow stretches the magnetic field lines which acquire a disk-like shape. Due to the conservation of angular momentum, the growth of the radial velocity of the plasma in the disk causes a slowdown of the azimuthal velocity, which lags from the rigid corotation. This leads to the operation of the unipolar induction. The unipolar induction creates a field-aligned current at a distance R_A associated with the divergence of azimuthal currents in the disk due to differential rotation. This current flows out from the upper atmosphere/ionosphere of the brown dwarf auroral oval into the disk. It is carried by precipitating electrons which increase the conductivity of the ionosphere where they enter it (Nichols et al., 2012). Nichols et al. (2012) noted that at Jupiter the conductivity of the ionosphere in the zone of the main ovals increases due to this effect by 1000 times.

We assume that an isolated ultra-cool brown dwarf has an atmosphere with minimal ionization of the upper layer – the ionosphere, due to possible corpuscular influence from the outside (see, for example, Helling et al., 2011a, b; Clement et al., 2024) or the thermal effect (Rodrıguez-Barrera et al., 2015). Helling and Rimmer (2019) noted that brown dwarfs are exposed to interstellar radiation. Rimmer and Helling (2013) showed that cosmic rays play a significant role in ionization of brown dwarfs' upper atmosphere. Brown dwarfs do not have moons, since they formed under the influence of gravitational collapse, like stars. For ionization by energetic particles, it is necessary that their energy is greater than the ionization energy of neutrals. Rodrıguez-Barrera et al. (2015), considering thermal ionization of the atmosphere of ultra-cool brown dwarfs, concluded that auroras are possible even without the presence of a flowing wind from a companion object or volcanic moons.

As a rough approximation, we assume following Hill (2001) and Nichols et al. (2012), that the magnetic field of W1935 is dipole with an axis perpendicular to the

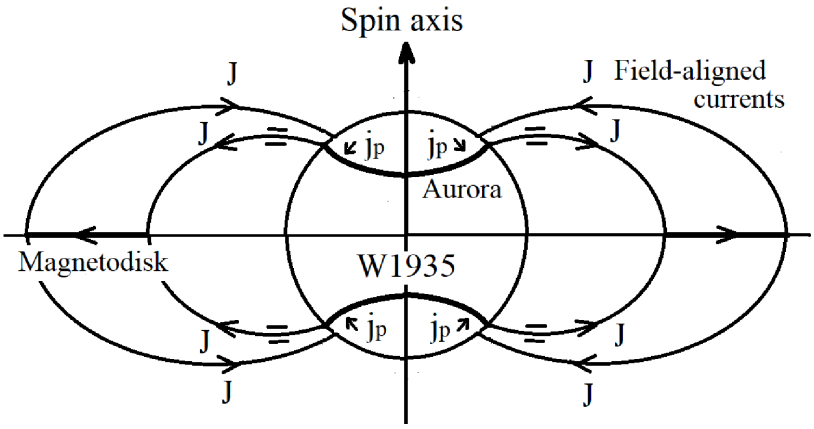


Figure 2 Current system of magnetodisk, including field-aligned currents J, magnetodisk currents and ionospheric Pedersen currents j_p. Current directions are shown by asterisks. Arcs are the auroral ovals at the brown dwarf.

disk and parallel to the rotation axis. Nichols et al. (2012) applied for ultra-cool brown dwarfs an axisymmetric model of the field-aligned currents distribution caused by unipolar induction, like that developed for Jupiter.

Nichols et al. (2012) pointed out that the generation of polar auroras requires the existence of an accelerating gap that accelerates electrons directed to the ionosphere to super thermal energies. In this case, for ultra-cool brown dwarfs, the relativistic theory should be used.

We suppose that one of the reasons for the occurrence of an accelerating gap above the ionosphere could be, for example, a large potential difference created by unipolar induction and a lack of the corresponding number of charges that carry strong field-aligned currents from the ionosphere of the brown dwarf to the plasma disk. In the current system, considered by us, there is a field-aligned current flowing out of the ionosphere at the auroral colatitude θ_{oval}, going to the equatorial disk (magnetodisk) at the Alfvén radius R_A and then spreading radially in the disk. At the outer edge of the disk, this current is closed by a field-aligned current flowing into the ionosphere, which is not associated with auroras. In the ionosphere this field-aligned current is linked by Pedersen current j_p with the outward from the ionosphere field-aligned current (see Fig. 2). In this current system there are two sliding contacts: on the ionosphere due to collisions of ions with neutrals and on the Alfvén radius in the equatorial disk due to the radial outflow of plasma, causing a lag from the rigid corotation (Belenkaya and Alexeev, 2021).

In the approximation of rigid corotation of magnetospheric plasma close to the brown dwarf ($r < R_A$), the electric field of corotation is determined by the formula:

$$\boldsymbol{E}_{rig} = -[\boldsymbol{\Omega}_{bd} \times \boldsymbol{r}] \times \boldsymbol{B}, \tag{1}$$

where $\boldsymbol{\Omega}_{bd}$ is the angular velocity of the brown dwarf rotation; $\boldsymbol{r}$ is the radius-vector from the center of brown dwarf; $\boldsymbol{B}$ is the magnetic field.

Electric potential corresponding to rigid corotation Φ_{rig} ($\boldsymbol{E}_{rig} = -\nabla\Phi_{rig}$) equals to (Belenkaya, 2004):

$$\Phi_{rig} = \frac{B_{bd}R_{bd}^3\Omega_{bd}\sin 2\theta}{r}, \tag{2}$$

where B_{bd} is the dipole magnetic field at the brown dwarf's equator; θ is the polar angle measured from the magnetic axis to the radius vector $\boldsymbol{r}$.

The electrical potential difference between the pole and the equator of a brown dwarf under assumption of rigid corotation by analogy with Jupiter (Belenkaya, 2004) is:

$$\Delta\Phi_{rig} = B_{bd}R_{bd}^2\Omega_{bd}. \tag{3}$$

Following Hill (2001), who studied the polar auroras in the main ovals of Jupiter, we can write an expression for the total power, which can be extracted from the rotation of brown dwarf:

$$P_0 = \frac{2\pi\Sigma_i B_{bd}^2\Omega_{bd}^2 R_{bd}^6}{R_A^2}, \tag{4}$$

where Σ_i is the effective ionospheric conductance of the brown dwarf which is a few times less than the integrated over the height of the conducting layer of ionospheric conductivity δ (δ is the conductivity tensor). We replaced in the denominator in our Eq. (4) the Hill's value L_0 (the radial distance in Jupiter's radii, at which rigid corotation breaks down in (Hill, 2001, Eq. (4)) by R_A/R_{bd}.

Taking into account Eq. (3), Eq. (4) can be rewritten as:

$$P_0 = 2\pi\Sigma_i\left(\frac{\Delta\Phi_{rig}R_{bd}}{R_A}\right)^2. \tag{5}$$

As noted above, the conductance in the oval Σ_i increases due to the precipitation of electrons carried by the field aligned current. These electrons must be additionally accelerated compared to thermal values. The numerator in the fraction in the expression for P_0 (Eq. (5)) depends only on the properties of the brown dwarf, and the denominator additionally on the characteristics of the circum-substellar plasma disk, as will be seen below.

As R_A is the distance in the magnetodisk, where Alfvén Mach number $M_A = \frac{V_{pl}}{V_A} = 1$, we can conclude that

$$\frac{\Omega_{bd}R_A(\mu_0 m_i n_i)^{1/2}}{B_{RA}} = 1, \tag{6}$$

where $V_{pl} = \Omega_{bd}R_A$ under the assumption of rigid corotation of plasma in the disk up to the distance R_A, and the Alfvén velocity $V_A = \frac{B_{RA}}{(\mu_0 m_i n_i)^{1/2}}$; here B_{RA} is the brown dwarf's magnetic field at R_A; μ_0 is the magnetic permeability of free space; m_i and n_i are the mass and density of the disk's ions, correspondingly.

As we assumed in the rough approximation that the brown dwarf's magnetic field is dipole, then B_{RA} can be determined from the equation:

$$B_\theta = \frac{B_{bd}R_{bd}^3\sin\theta}{r^3}. \tag{7}$$

At the Alfvén radius in the equatorial plane, $\theta = 90^\circ$ and $r = R_A$. Thus,

$$B_{RA} = B_{bd}\left(\frac{R_{bd}}{R_A}\right)^3. \tag{8}$$

Inserting B_{RA} from equation (8) into equation (6), we obtain:

$$\frac{\Omega_{bd} R_A^4 (\mu_0 m_i n_i)^{1/2}}{B_{bd} R_{bd}^3} = 1, \tag{9}$$

or

$$R_A^4 = \frac{B_{bd} R_{bd}^3}{\Omega_{bd} (\mu_0 m_i n_i)^{1/2}}. \tag{10}$$

Inserting R_A into equation (5), we have:

$$P_0 = 2\pi \Sigma_i \left(\Delta\Phi_{rig}\frac{R_{bd}}{R_A}\right)^2 = 2\pi\Sigma_i(\Delta\Phi_{rig})^2 \frac{\left[R_{bd}\Omega_{bd}(\mu_0 m_i n_i)^{1/2}\right]^{1/2}}{(B_{bd})^{1/2}} \tag{11}$$

or

$$P_0 = 2\pi\Sigma_i(\Delta\Phi_{rig})^2 \left(\frac{\Omega_{bd} R_{bd}}{B_{bd}}\right)^{1/2} (\mu_0 m_i n_i)^{1/4} \tag{12}$$

and

$$P_0 = 2\pi\Sigma_i (B_{bd}\Omega_{bd} R_{bd}^2)^2 \left(\frac{\Omega_{bd} R_{bd}}{B_{bd}}\right)^{1/2} (\mu_0 m_i n_i)^{1/4} = 2\pi\Sigma_i B_{bd}^{3/2} \Omega_{bd}^{5/2} R_{bd}^{9/2} (\mu_0 m_i n_i)^{1/4}. \tag{13}$$

Thus, the total power, which can be extracted from the brown dwarf's rotation, P_0, is expressed by its parameters and parameters of the surrounding plasma disk.

Part of the energy coming to the oval of the fast-rotating ultra-cool magnetic brown dwarf from the surrounding plasma disk can be emitted in the radio diapason. If the possible relevant radiation is circularly polarized, it must be generated by CMI.

Zarka (2007) noted that the "radio-magnetic Bode law" shows what part of the incident flux, P_{input}, can be emitted in the radio diapason P_{Radio}:

$$P_{Radio} \sim \eta P_{input}, \tag{14}$$

where $\eta << 1$. For the case of the isolated brown dwarf with the surrounding plasma disk, P_{input} is roughly characterized by P_0 (Eqs. (11–13)), being some part of it: $P_{input} \sim \eta_1 P_0$. So, the power extracted from rotation could be the energetic source of the brown dwarf's possible radio (and infrared) emissions.:

$$P_{Radio} \sim \eta\eta_1 P_0. \tag{15}$$

6 Ohmic heating

The strong field-aligned current flowing from the auroral ionosphere is connected with the Pedersen current spreading over the ionosphere with the surface density j_p. This Pedersen current produces heat q in the conductive layer of the ionosphere. Hill (2001) estimated the part of the power P_0 going to heating the Jovian ionosphere to be 39%. Goodman (2004), considering the efficiency of heating during the dissipation of the Pedersen current from the photosphere to the lower corona of the Sun, noted that a necessary condition for the efficiency of the dissipation of the Pedersen current is: $\sigma_p << \sigma_{||}$, where σ_p is the Pedersen conductivity, and $\sigma_{||}$ is the field-aligned conductivity along the magnetic field (the Hall current is non-dissipative).

The brown dwarf's ionospheric current can heat the atmosphere by ohmic dissipation or Joule heating, the rate of which is proportional to the current flowing along the electric field – the Pedersen current. The Hall current, perpendicular to the magnetic and electric fields, does not participate in ohmic dissipation. The rate of Joule heating integrated over the height of the ionospheric conductive layer is (Baumjohann and Treumann, 1996):

$$Q_J = J_\perp \times \boldsymbol{E}_\perp = \Sigma_P \times \boldsymbol{E}_\perp^2, \tag{16}$$

where $J_\perp = \Sigma_P \times \boldsymbol{E}_\perp$ is the ionospheric Pedersen current density integrated over the height of conducting layer, h; $\Sigma_P = \int \sigma_p \partial h$ is the ionospheric Pedersen conductivity integrated over height h, and $\boldsymbol{E}_\perp$ is the electric field perpendicular to the magnetic field. Conductivity is greater in the upper layer of the atmosphere/ionosphere, where precipitating energetic particles from the auroral field-aligned current increases it, so more heat is released there than in the lower layers. The specific properties of the brown dwarf's atmosphere determine where exactly the conductivity is highest and where, correspondingly, the most heat is released. In the Earth's ionosphere, this layer is called the dynamo layer. In the dynamo region, electrons are magnetized $(\omega_e/\nu_e)^2 >> 1$, but ions are not (ω_e is the electron gyrofrequency, and ν_e is the frequency of electron collisions with ions and neutrals).

The Pedersen conductivity σ_p is expressed in terms of the electron cyclotron frequency $\omega_{ge} = \dfrac{eB}{m_e}$ and ion cyclotron frequency $\omega_{gi} = \dfrac{zeB}{m_i}$, where z is the charge number, the frequencies of electron-neutral collisions ν_{en} and ion-neutral collisions ν_{in}, if there is only one type of ions in the ionosphere (Baumjohann and Truman, 1996):

$$\sigma_p = \left(\frac{\nu_{en}}{\nu_{en}^2 + \omega_{ge}^2} + \frac{m_e}{m_i} \frac{\nu_{in}}{\nu_{in}^2 + \omega_{gi}^2} \right) \frac{n_e e^2}{m_e}. \tag{17}$$

Thus, at a certain altitude determined by the properties of the brown dwarf's atmosphere, there is a conductive current layer in which heat is released at a rate proportional to the integral Pedersen conductivity (Eq. (16)). This heat spreads deeper into the atmosphere, creating a temperature inversion. In this case, the maximum ionospheric conductivity should be in the upper layer, in the auroral zone due to the precipitation of accelerated electrons there.

The hypothesis we have adopted about the existence of a plasma current disk surrounding the ultra-cool brown dwarf W1935, possessing magnetic field, allows us to explain the observed infrared emission and temperature inversion with atmospheric

height for this object, while for its twin, the isolated brown dwarf W2220, the supposed absence of the intrinsic magnetic field and/or surrounding plasma disk also explains the absence of similar observations.

Unfortunately, we have no data on the parameters of the plasma surrounding these two isolated ultra-cool sub-brown dwarfs, which prevents us from making any estimates. This paper presents only a possible explanation for the observations described by Faherty et al. (2024).

7 Conclusions

Studying the temperature-density relationship for M-class stars, brown dwarfs and giant planets allowed us to trace the evolution of sub-stellar celestial bodies with time. It occurred that for the brown dwarfs of M class the temperature was approximately constant ∼2000–2300 K while the density increased from 0.2 to 200 g/cm^3. Only starting from L to Y classes the temperature and density of brown dwarfs decreased with age from ∼2000 K to ∼300 K and from ∼200 g/cm^3 to ∼15 g/cm^3. Two twin ultra-cool brown dwarfs, which we studied here, are located at the end of the obtained evolution trajectory for the sub-stellar objects.

The purpose of this paper is to find an answer to the question: why one of two twin isolated ultra-cool brown dwarfs exhibited auroras and temperature inversion with atmospheric altitude, while the other did not. We suggest that a possible reason is that one brown dwarf (W1935) has a magnetic field and a surrounding plasma magnetodisk. When the magnetic dwarf rotates rapidly, the interaction with the magnetodisk can cause the observed phenomena. If the second brown dwarf (W2220) does not have its own magnetic field and/or magnetodisk, it does not have the necessary conditions for generating aurora and it does not have a temperature inversion with atmospheric altitude. We show how these phenomena depend on the brown dwarf characteristics and parameters of the circum-substellar plasma disk.

The study was conducted under the state assignment of Lomonosov Moscow State University.

References

Alexeev, I.I. and E. S. Belenkaya, Alfvén wings in the vicinity of a conducting body in a magnetized plasma, Journal of Atmospheric and Solar-Terrestrial Physics. 53. 11/12. pp. 1099-1101. 1991. https://doi.org/10.1016/0021-9169(91)90058-F

Alexeev I.I. Belenkaya E.S., Modeling of the Jovian Magnetosphere. Annales Geophysic, 23, 809-826, 2005. https://doi.org/10.5194/angeo-23-809-2005, 2005

Baumjohann, W., R.A. Treumann, Basic Space Plasma Physics, Imperial College Press, 1996. DOI: 10.1142/p015

Belenkaya, E.S. The Jovian magnetospheric magnetic and electric fields: Effects of the interplanetary magnetic field, Planetary and Space Science, 52, 499-511, 2004. DOI: 10.1016/j.pss.2003.06.008

Belenkaya Elena, Khodachenko Maxim, Accretion and current discs controlled by strong magnetic field, International Journal of Astronomy and Astrophysics, 2, 81-96, 2012, doi: 10.4236/ijaa.2012.22012

Belenkaya E., Alexeev I., Sliding Contacts in Planetary Magnetospheres, Symmetry, MDPI, 13, № 2: 283, 2021. https://doi.org/10.3390/sym13020283

Bespalov, Peter A., Olga N. Savina, An excitation mechanism of electromagnetic pulses by relativistic electrons in the brown dwarfs rarefied magnetosphere, MNRAS, 480, 4761–4765, 2018. https://doi.org/10.1093/mnras/sty2204

Clement, Noe, Yuki Nakamura, Michel Blanc, Yuxian Wang, Sariah Al Saati, Ionospheric conductances at the giant planets of the Solar System: a comparative study of ionization sources and the impact of meteoric ions, arXiv:2412.04219, 2024. https://doi.org/10.48550/arXiv.2412.04219

Climent, J. B., J. C. Guirado, J. M. Marcaide, L. Peña-Moñino, Evidence for a radiation belt around a brown dwarf, Science, 381, No. 6662, 2023, DOI: 10.1126/science.adg6. https://doi.org/10.48550/arXiv.2303.06453

Cowley, S. W. H., E. J. Bunce, J. D. Nichols, Origins of Jupiter's main oval auroral emissions, JGR, 108, A4, 2003, doi: 10.1029/2002JA009329

Cushing C. Michael, J. Davy Kirkpatrick, Christopher R. Gelino, Roger L. Griffith, Michael F. Skrutskie, A. Mainzer, Kenneth A. Marsh, Charles A. Beichman, Adam J. Burgasser, Lisa A. Prato, The discovery of y dwarfs using data from the wide-field infrared survey explorer (WISE), ApJ, 743:50 (17pp), 2011. DOI: 10.1088/0004-637X/743/1/50

Faherty, Jacqueline K., Ben Burningham, Jonathan Gagn´e, Genaro Su´arez, Johanna M. Vos, Sherelyn Alejandro Merchan, Caroline V. Morle, Melanie Rowland, Brianna Lacy, Rocio Kiman, Dan Caselden, J. Davy Kirkpatrick, Aaron Meisner, Adam C. Schneider, Marc Jason Kuchner, Daniella Carolina Bardalez Gagliuffi, Charles Beichman Peter Eisenhardt, Christopher R. Gelino, Ehsan Gharib-Nezhad, Eileen Gonzales, Federico Marocco, Austin James Rothermich, Niall Whiteford, Methane emission from a cool brown dwarf. Nature, 628, 511–514, 2024. https://doi.org/10.1038/s41586-024-07190-w

Gerasimov, Roman, Luigi R. Bedin, Adam J. Burgasser, Daniel Apai, Domenico Nardiello, Efrain Alvarado, Jay Anderson, JWST Imaging of the Closest Globular Clusters. II. Discovery of Brown Dwarfs in NGC 6397 and Measurement of Age from the Brown Dwarf Cooling Sequence, Using SANDee—A New Grid of Model Isochrones across the Hydrogen-burning Limit, ApJ. 971, 65, pages 12. 2024. DOI: 10.3847/1538-4357/ad5551

Goodman, M. L., On the efficiency of plasma heating by Pedersen current dissipation from the photosphere to the lower corona, A&A, 416, 115 9–1178, 2004. DOI: 10.1051/0004-6361:20031719

Hallinan, G. A. Antonova, J. G. Doyle, S. Bourke, C. Lane, and A. Golden, Confirmation of the electron cyclotron maser instability as the dominant source of radio emission from very low mass stars and brown dwarfs, ApJ, 684:644Y653, 2008. DOI: 10.1086/590360

Helling Ch, Rimmer P.B. Lightning and charge processes in brown dwarf and exoplanet atmospheres. Phil. Trans. R. Soc. A 377: 20180398. 2019 http://dx.doi.org/10.1098/rsta.2018.0398

Helling, Ch., M. Jardine, S. Witte, D. A. Diver, Ionization in atmospheres of brown

dwarfs and extrasolar planets. I. The role of electron avalanche, ApJ, 727:4 (6pp), 2011a, doi:10.1088/0004-637X/727/1/4

Helling, Ch., M. Jardine, F. Mokler, Ionization in atmospheres of brown dwarfs and extrasolar planets. II. Dust-induced collisional ionization, ApJ, 737:38 (11pp), 2011b, doi:10.1088/0004-637X/737/1/38

Hill, T. W., Corotation lag in Jupiter's magnetosphere: Comparison of observation and theory, Science, 207, 301, 1980. DOI: 10.1126/science.207.4428.3

Hill, T.W., The Jovian auroral oval, JGR, 106, A5, 8101-8108, 2001, DOI: 10.1029/2000JA000 302

Kao, Melodie M,. Gregg Hallinan, J. Sebastian Pineda, David Stevenson, and Adam Burgasser, The strongest magnetic fields on the coolest brown dwarfs, The Astrophysical Journal Supplement Series, 237:25 (25pp), 2018. https://doi.org/10.3847/1538-4365/aac2d5

Khodachenko, M. L., Alexeev, E. Belenkaya, H. Lammer, J.-M. Grießmeier, M. Leitzinger, P. Odert, T. Zaqarashvili, H. O. Rucker, Magnetospheres of "hot jupiters": The importance of magnetodisks in shaping a magnetospheric obstacle, ApJ, 744:70 (16pp), 2012. doi:10.1088/0004-637X/744/1/70

Kivelson, M. G., K. K. Khurana, C. T. Russell, R. J. Walker, J. Warnecke, F. V. Coroniti, C. Polanskey, D. J. Southwood, G. Schubert, Discovery of Ganymede's magnetic field by the Galileo spacecraft, Nature, 384, 537–541, 1996. DOI: 10.1038/384537a0

Kobyakov, D., Some properties of plasma surrounding brown dwarfs, arXiv:210.18017 v1, 2023. https://doi.org/10.48550/arXiv.2310.18017

Luhman, K. L, Discovery of a 250 K brown dwarf at 2 pc from the Sun, The Astrophysical Journal Letters. 786:L18, 6pp. 2014. DOI: 10.1088/2041-8205/786/2/L18

Nakajima, R., The circumstellar gas of sigma orionis E, Astrophysics and Space Science, 116, 285–297, 1985

Neubauer, F.M., Nonlinear standing Alfvén wave current system at Io: Theory, JGR, 85, A3, 1171-1178, 1980. https://doi.org/10.1029/JA085iA03p01171

Nichols, J. D., S. E. Milan, Stellar wind–magnetosphere interaction at exoplanets: computations of auroral radio powers, MNRAS, 461, 2353–2366, 2016. doi:10.1093/mnras/stw1430.

Nichols, J. D., M. R. Burleigh, S. L. Casewell, S. W. H. Cowley, G. A. Wynn, J. T. Clarke, A. A. West, Origin of electron cyclotron maser induced radio emissions at ultracool dwarfs: Magnetosphere–ionosphere coupling currents, ApJ, 760:59 (9pp), 2012. doi:10.1088/0004-637X/760/1/59

Persson M. Carina, Szilárd Csizmadia, Alexander J. Mustill, Malcolm Fridlund, Artie P. Hatzes, Grzegorz Nowak, Iskra Georgieva, Davide Gandolfi, Melvyn B. Davies, John H. Livingston, Enric Palle, Pilar Montañes Rodríguez, Michael Endl, Teruyuki Hirano, Jorge Prieto-Arranz, Judith Korth, Sascha Grziwa, Massimiliano Esposito, Simon Albrecht, Marshall C. Johnson, Oscar Barragán, Hannu Parviainen, Vincent Van Eylen, Roi Alonso Sobrino, Paul G. Beck, Juan Cabrera, Ilaria Carleo, William D. Cochran, Fei Dai, Hans J. Deeg, Jerome P. de Leon, Philipp Eigmüller, Anders Erikson, Akai Fukui, Lucía González-Cuesta, Eike W. Guenther, Diego Hidalgo, Maria Hjorth, Petr Kabath, Emil Knudstrup, Nobuhiko Kusakabe, Kristine W. F. Lam, Mikkel N. Lund, Rafael Luque, Savita Mathur, Felipe Murgas, Norio Narita, David Nespral, Prajwal Niraula, A. O. Henrik Olofsson, Martin Pätzold,

Heike Rauer, Seth Redfield, Ignasi Ribas, Marek Skarka, Alexis M. S. Smith, Jan Subjak, Motohide Tamura, Greening of the Brown Dwarf Desert, A&A 628, A64, 2019. https://doi.org/10.1051/0004-6361/201935505

Reiners, A., U. R. Christensen, A magnetic field evolution scenario for brown dwarfs and giant planets, A&A, 522, A13, 2010. DOI: 10.1051/0004-6361/201014251

Rimmer, P. B., Ch. Helling, Ionization in atmospheres of brown dwarfs and extrasolar planets. IV. The effect of cosmic rays. ApJ, 774:108 (10pp), 2013. doi:10.1088/0004-637X/774/2/108

Robbins, Grady, Aaron M. Meisner, Adam C. Schneider, Adam J. Burgasser, J. Davy Kirkpatrick, Jonathan Gagne, Chih-Chun Hsu, Leslie Moranta, Sarah Casewell, Federico Marocco, Roman Gerasimov, Jacqueline K. Faherty, Marc J. Kuchner, Dan Caselden, Michael C. Cushing, Sherelyn Alejandro, CWISE J105512.11+5443 28.3: A nearby Y dwarf spectroscopically confirmed with Keck/NIRES, ApJ. 958:94 (11pp). 2023. DOI: 10.3847/1538-4357/ad0043

Rodrıguez-Barrera, M. I., Ch. Helling, C. R. Stark, A. M. Rice, Reference study to characterise plasma and magnetic properties of ultra-cool atmospheres, MNRAS, 454, 3977–3995, 2015. doi:10.1093/mnras/stv2090

Saur, Joachim, Clarissa Willmes, Christian Fischer1, Alexandre Wennmacher, Lorenz Roth, Allison Youngblood, Darrell F. Strobel, Ansgar Reiners, Brown dwarfs as ideal candidates for detecting UV aurora outside the Solar System: Hubble Space Telescope observations of 2MASS J1237+6526, A&A, 655, A75, 2021. https://doi.org/10.1051/0004-6361/202040230

Scholz, Aleks, Keavin Moore, Ray Jayawardhana, Suzanne Aigrain, Dawn Peterson, Beate Stelzer, A universal spin-mass relation for brown dwarfs and planets, ArXiv:180.0730v2, 2018. https://doi.org/10.48550/arXiv.1804.07380

Wright, A. N., D. J. Southwood, Stationary Alfvénic structures, JGR, 92, A2, 1167-1175, 1987. https://doi.org/10.1029/JA092iA02p01167

Zarka, P., Plasma interactions of exoplanets with their parent star and associated radio emissions, Planetary and Space Science, 55, 598–617, 2007. DOI: 10.1016/j.pss.2006.05.045